Optics Letters

Compact high-contrast silicon optical filter using all-passive and CROW Fano nanobeam resonators

Ziwei Cheng,[1,2,†] Jiahui Zhang,[1,†] Jianji Dong,[1,3] and Yunhong Ding[2,4]

[1]Wuhan National Laboratory for Optoelectronics, School of Optical and Electronic Information, Huazhong University of Science and Technology, Wuhan, 430074, China
[2]Department of Photonics Engineering, Technical University of Denmark, DK-2800 Kongens Lyngby, Denmark
[3]e-mail: jjdong@hust.edu.cn
[4]e-mail: yudin@fotonik.dtu.dk

Received 10 June 2021; revised 13 July 2021; accepted 13 July 2021; posted 13 July 2021 (Doc. ID 433850); published 5 August 2021

We propose and experimentally demonstrate a high-order coupled-resonator optical waveguide (CROW) nanobeam filter with semi-symmetrical Fano resonance enhancement. Thanks to the tight arrangement of multiple nanobeams and assistance of the partial transmission element, the designed filter has a high-contrast transmission and low insertion loss. Finally, the fabricated filter has a compact size of 20 μm × 10 μm, a high extinction ratio as much as 70 dB, and an insertion loss as low as 1 dB. This filter shows a passive structure without thermal control configuration for calibration on each resonator. This compact filter can be a basic building block for various applications requiring high extinction ratio filtering, such as single-photon source filtering of integrated photon chips.

https://doi.org/10.1364/OL.433850

Filters are one of the main functional devices of integrated photonics technology, which have important applications in various optical fields such as spectral analysis, nonlinear optical wavelength conversion, and wavelength-division multiplexing (WDM) [1,2]. For instance, optical quantum computing and communication use a single photon with low light field intensity as the basic quantum, which thus requires a filter device to effectively extract weak single-photon signals from noise [3–5]. On the one hand, all kinds of single-photon sources basically produce a single photon by using strong pump light. So, as to prevent the sensitive single-photon detector from being affected by the pump light, high extinction ratio filters are necessarily indispensable. On the other hand, for reducing the loss of a single photon, filters used in the integrated optical quantum chip need to achieve a lower insertion loss compared to the classical optics. In order to meet the demand for high extinction ratio filtering, traditional bulky optics solutions such as cascaded fiber Bragg gratings and benchtop optical filtering equipment are generally used. These methods not only bring high single-photon loss, but also reduce the integration level of the chip. Mach–Zehnder interferometer (MZI) devices have certain filtering capabilities, and many high extinction ratio filter solutions based on cascaded MZI have been proposed [6,7]. However, the passband bandwidth of the MZI unit device is relatively wide, and the size of the multi-unit cascade is too large, so there are many limitations in practical applications. The integrated photonic resonant device, such as a microring, is a natural narrow-band filter. However, the extinction ratio of a single resonant device is generally not high enough, and multiple devices need to be coupled to improve the performance [8]. Although a single microring is more compact than the MZI structure, it still covers a larger size in the case of high-order connection [9–11]. In order to cope with the deviation caused by the manufacturing process and make each resonator work in an aligned wavelength, each resonant unit of these filters needs to be assisted by active tuning, which not only further increases the size, but also brings additional energy consumption and difficulty in control and thermal crosstalk [12–15].

In this Letter, we propose a compact and high-contrast optical filter using high-order coupled-resonator optical waveguide (CROW) nanobeam cavities enhanced by Fano resonance. The one-dimensional photonic crystal nanobeam structures contribute to a compact device size of 20 μm × 10 μm. Multiple nanobeams are tightly arranged and coupled to form a high-order resonant cavity to perform filtering with an extinction ratio as high as 70 dB, and it has a very wide stop band, which is not limited by free spectral range (FSR). The semi-symmetrical Fano structure improves the transmission efficiency and effectively reduces the insertion loss to as low as 1 dB. The narrow spacing minimizes the process error between the nanobeams, so the device does not require separate thermal tuning and calibration. Benefiting from advantages on fabrication and integration with the complementary metal oxide semiconductor (CMOS) compatible process, it has potential applications in on-chip high extinction ratio filtering.

Figure 1(a) is a schematic of a high-order nanobeam resonator filter, whose basic unit is a high quality (Q) factor nanobeam resonator. This structure achieves resonance by introducing defects in a one-dimensional photonic crystal. Because the nanobeams are shaped like an ordinary waveguide, the order of nanobeams can be effectively increased while keeping the overall size very small when they are tightly arranged in the lateral direction. As a consequence, the process deviation between nanobeams is minimized, so it is no longer necessary to individually tune and calibrate each resonator like a high-order microring structure,

which greatly reduces the structural complexity and footprint. Figure 1(b) is a partial schematic of the filter. The main parameters of each nanobeam unit are ellipse hole horizontal axis diameter h_x, longitudinal axis diameter h_y, period a, nanobeam width w, and coupling distance d. The increase in the size of the holes (h_x and h_y) or the decrease in the period a and nanobeam width w will make the effective refractive index smaller, and therefore the central wavelength will shift to a shorter wavelength. A tapered structure with gradually changing parameters is set between the photonic crystal on both sides ($h_x = 259$ nm and $h_y = 275$ nm) and the etched hole structure in the center of the resonator ($h_x = 250$ nm and $h_y = 180$ nm), which allows a smooth transition and reduces the loss. Figure 1(c) shows the energy band gap from the center to the holes at both ends. Here, we define *aspect ratio* to reflect the change of the hole size, and its value is h_y/h_x. Note that the energy bands here are designed for the transverse electric (TE) mode, and only the band gap information is retained, which is the area between the red and blue lines in Fig. 1(c). It can be seen that as the structural parameters change, and the upper energy band intersects with the dashed line corresponding to the 1550 nm wavelength. This means that the optical field with a wavelength of 1550 nm at the center elliptical hole has a mode whose wave vector has its main component along the axial direction. Since the dashed line is in the band gap of the edge holes, the light field will be reflected, thus forming resonance. Note that there is also a gradual change in the period a from 372.7 nm to 437.5 nm, so the energy band increases to a lager value as the hole size changes. Due to the low transmission efficiency of the nanobeam as a four-port unit device, the insertion loss will increase unacceptably when the order increases. To this end, we need to introduce the partial transmission element (PTE) to achieve semi-symmetric Fano resonance [16]. Similarly, the introduction of one-dimensional photonic crystal etched holes on the coupling waveguide, as is shown in Fig. 1(b), can easily achieve this point. Its property can be changed by adjusting the parameters of the holes. According to the temporal coupled-mode theory analysis of the structure [16,17], an output transfer function can be obtained, shown as follows:

$$T_{\text{out}}(\omega) = \frac{4\gamma_1^2}{|j(\omega_0 - \omega) + 2\gamma_1 + 2\gamma_2 + \gamma_v|^2}, \tag{1}$$

$$\max(T_{\text{out}}) = \frac{4}{\left(2 + \frac{2}{\left(\frac{\gamma_1}{\gamma_2}\right)} + \frac{\gamma_v}{\gamma_1}\right)^2}, \tag{2}$$

$$\frac{1-r}{1+r} \le \frac{\gamma_1}{\gamma_2} \le \frac{1+r}{1-r}, \tag{3}$$

where ω_0 is the central frequency of the resonance, γ_1 and γ_2 are the cavity decay rate to each port in the semi-symmetric structure, while γ_v is the intrinsic loss of the nanobeam. Without the semi-symmetrical Fano resonant structure, the value of the energy loss ratio γ_1/γ_2 is not maximized, and the maximum value of the output function will be very small. This makes the extinction ratio of the Lorentz filter lineshape very low and causes great insertion loss as well. To achieve the maximum value of γ_1/γ_2 and to obtain the highest transmission efficiency, it can be seen from Eq. (3) that γ_1/γ_2 is limited by the reflectivity r of the PTE. Therefore, the reflectivity of the PTE should be made as large as possible. Enough photonic crystal holes are introduced to the coupling waveguide so the reflectivity r is equal to one, and it constitutes a high-output rotationally symmetric Fano resonant structure. Furthermore, we also optimized the overall position of the PTE structure in the horizontal direction to maximize γ_1/γ_2, resulting in low insertion loss. A gradient design is also introduced at the coupling end of the PTE to reduce the scattering loss caused by the incident light field.

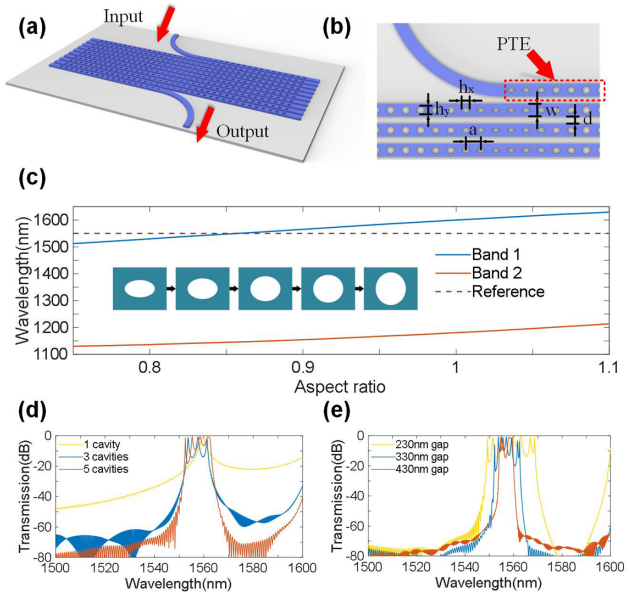

Fig. 1. (a) Schematic of the proposed CROW nanobeam filter. (b) Partial view and main parameters. (c) Photonic band gap of tapered etching holes. Simulation of transmission spectrum of devices with (d) different orders and (e) different coupling distance d.

On the basis of the enhancement of the transmission efficiency by the semi-symmetrical Fano resonance, the order of the nanobeam resonant cavities can be further improved to achieve a higher extinction ratio. According to the CROW theory [18,19], the number of nanobeam resonant cavities is increased to 3 and 5 under the premise of the same cavity structure. Three-dimensional finite difference time-domain (3D-FDTD) simulation is performed. The transmission spectra of the three structures obtained are shown in Fig. 1(d). As the order of nanobeams increases, the extinction ratio of the filter can also improve. The extinction ratio of the first-order nanobeam resonator filter can reach 40 dB, the third-order one is about 60 dB, and the extinction ratio is even higher than 70 dB after being upgraded to the fifth-order. In addition, the peaks of the transmission spectrum increase due to multi-cavity coupling, which also makes the transmission spectrum wider [20]. Therefore, the cavity distance d needs to be optimized to appropriately reduce the inter-cavity coupling and make the peaks of the transmission spectrum more concentrated. We further simulated the seventh-order nanobeam resonator filter with nanobeam distance of 230 nm, 330 nm, and 430 nm, and the transmission spectrum is shown in Fig. 1(e). Assume that the order of the nanobeam resonant cavity is unchanged, and then the obtained extinction ratio remains constant, which is basically between 70–80 dB. However, as the distance between the nanobeams increases, the multiple peaks of the transmission spectrum become more and more concentrated, and the passband of the transmission spectrum becomes narrower. In

Fig. 2. Scanning electron microscope (SEM) image of (a) Fano resonance enhanced ninth-order nanobeam filter, (b) coupling area, and (c) photonic crystal grating.

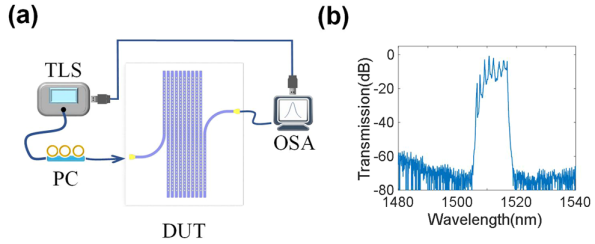

Fig. 3. (a) Schematic of the experimental setup. (b) Transmission spectrum of the actual device. TLS, tunable laser source; PC, polarization controller; DUT, device under test; OSA, optical spectrum analyzer.

addition, the high-order nanobeam filter has a wide high extinction ratio stop band, and it is even capable for multi-frequency or broad-spectrum noise without FSR limit.

The fabrication started from the standard CMOS process based on the silicon-on-insulator (SOI) platform, where the electron beam lithography (EBL) and inductively coupled plasma (ICP) were executed in sequence. The obtained scanning electron microscope (SEM) image of the ninth-order nanobeam resonator filter structure is shown in Fig. 2(a). The deviation introduced by manufacturing process is almost the same among the various nanobeam resonant cavities. As a result, the resonant frequency, Q factor, and other parameters of cavities remain consistent, which ensures the realization of the filter design. The main impact of deviation is only the drift of the overall passband spectrum. Figures 2(b) and 2(c) are a partial view of the device and the photonic crystal grating coupler, respectively. In order to eliminate the loss of grating couplers and waveguides, we also fabricated some identical grating couplers directly linked to straight waveguides without nanobeam resonators as references.

The completed device was tested by an experimental setup in Fig. 3(a). The light source from the tunable laser source (TLS) is synchronized with the optical spectrum analyzer (OSA) in the output, and the measured spectrum is plotted in Fig. 3(b). The transmission spectra of a batch of comparative structures without nanobeams had been tested in advance, and then they were subtracted. The results are shown in Fig. 3(b). One can see that the ninth-order nanobeam resonator filter achieved an ultra-high extinction ratio of about 70 dB. This is achieved only

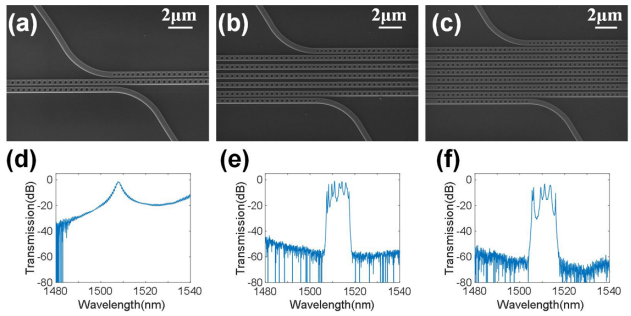

Fig. 4. SEM image of (a) first-order, (b) fifth-order, and (c) seventh-order nanobeam filter. (d), (e), and (f) Corresponding transmission spectrum of (a), (b), and (c), respectively.

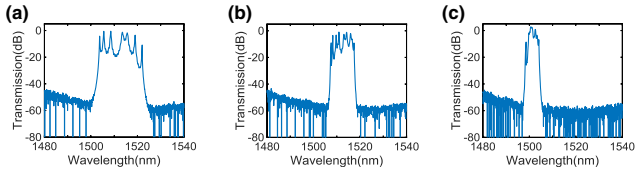

Fig. 5. Transmission spectrum of the seventh-order nanobeam filter with the coupling distances of (a) 230 nm, (b) 330 nm, and (c) 430 nm.

with the compact size of about 20 μm × 10 μm, which is only equivalent to the size of an ordinary microring, and the structure does not have any active control configuration to calibrate each resonator. The insertion loss of the nanobeam resonator filter is as low as 1 dB due to the lower energy loss of the nanobeam resonator itself, as well as the semi-symmetric Fano structure. One can see ripples in the passband, which is caused by multi-cavity coupling, and they can be restrained by weakening the coupling between nanobeams (a larger d). We have compared the performance with other on-chip integrated filters in Table 1.

This result has an obvious advantage over other high-order resonator filtering demonstrations for a compact footprint and passive structure, which is of great significance in applications such as single-photon source filters. Note that the lowest detected optical power is already the lower limit that the spectrometer can detect, so the ninth-order filter is likely to have better filtering performance.

To study the influence of order and coupling strength on the performance of the filter, we also constructed resonant cavity filters with different orders and different coupling distances. The results are shown in Figs. 4 and 5, respectively.

On the one hand, for nanobeam filters of different orders, resonant cavity structure and coupling parameters are completely consistent. Figure 4 shows the SEM images and transmission spectra of the first-, fifth- and seventh-order nanobeam filters, respectively. The transmission of the single nanobeam filter is a

Table 1. Performance Comparison of Integrated Filter Work

Type	Order	Extinction Ratio (dB)	Insertion Loss (dB)	Unit Size (μm)	Individual Tuning	FSR Limit
MZI [7]	6	∼55	∼1.5	-	Yes	Yes
CROW microring [20]	4 + 4	110	∼3	Radius ∼ 10	Yes	Yes
CROW microring [21]	4	∼96	0.8	Radius ∼ 13.5	Yes	Yes
Bragg filters [22]	4	>60	2	∼1 × 300	Yes	Yes
This work	9	∼70	∼1	∼0.5 × 20	No	No

Lorentzian lineshape. For the fifth- and seventh-order devices, the edge of the passband is steep, which results in a square-wave filter. The biggest difference is that the extinction ratio of the single nanobeam filter is very low, while the fifth- and seventh-order filters can be increased to about 60 dB, and the aforementioned ninth-order filter can reach 70 dB. In addition, owing to the ultra-small size of the nanobeams and the Fano enhanced resonance effect, it is still theoretically possible to achieve a higher extinction ratio by increasing the order. Note that, as the order increases, each unit may not work at the same wavelength due to the fabrication deviation.

On the other hand, we have constructed seventh-order nanobeam resonator filters with nanobeam resonant cavity coupling distances of 230 nm, 330 nm, and 430 nm. Figure 5 illustrates the transmission spectra of the filter with a designed d of 230 nm, 330 nm, and 430 nm. It can be seen that as the coupling distance increases, multiple peaks of the transmission spectrum become more and more concentrated, and the passband width is further narrowed, which is consistent with the expectation of the simulation results. Therefore, the passband width of the actual structure can be adjusted by different coupling distances.

The fabricated device has a relatively larger hole size than the layout we designed because of the deviation of ICP etching process. This deviation is not uniform in different areas of the layout. This is the main reason for the different shift to a shorter wavelength for different devices. But, in a single device, this influence can be considered equal to all units, so the deviation is only shown as the overall shift of the passband spectra and does not affect the realization of the high extinction ratio filtering. To solve this problem, some error compensation should be made in advance. Otherwise, if necessary, it is easy to calibrate by using a single metal thermal electrode or other temperature control modules across all nanobeams, rather than tuning every unit individually, and it will basically not affect other characteristics such as extinction ratio.

Based on the enhancement effect of the semi-symmetrical PTE structure, the nanobeam resonant cavity has broken the bottleneck of transmission efficiency and shown great capabilities. We have realized an integrated photonic filter with high extinction ratio and low loss, which provides outstanding performance and extremely small size. The high-order nanobeam resonator filter has an extremely compact size of only about 20 μm × 10 μm and a simple structure that does not require active tuning and calibration of each resonator unit. It achieves an extinction ratio as high as 70 dB and an insertion loss as low as 1 dB. The device has a very wide stop band and is not limited by FSR. Our work can play an important role in a variety of on-chip high extinction ratio filtering applications and has the potential to be used in single-photon source filtering applications in integrated optical quantum platforms.

Funding. National Natural Science Foundation of China (61805090, 62075075); The Center of Excellence, Denmark SPOC (DNRF123); VILLUM FONDEN, QUANPIC (00025298).

Disclosures. The authors declare no conflicts of interest.

Data Availability. Data underlying the results presented in this paper are not publicly available at this time but may be obtained from the authors upon reasonable request.

[†]These authors contributed equally to this Letter.

REFERENCES

1. Y. Liu, A. Choudhary, D. Marpaung, and B. J. Eggleton, Adv. Opt. Photon. **12**, 485 (2020).
2. D. A. B. Miller, Proc. IEEE **97**, 1166 (2009).
3. D. Grassani, S. Azzini, M. Liscidini, M. Galli, M. J. Strain, M. Sorel, J. E. Sipe, and D. Bajoni, Optica **2**, 88 (2015).
4. R. R. Kumar, M. Raevskaia, V. Pogoretskii, Y. Q. Jiao, and H. K. Tsang, Appl. Phys. Lett. **114**, 5 (2019).
5. J. W. Silverstone, D. Bonneau, J. L. O'Brien, and M. G. Thompson, IEEE J. Sel. Top. Quantum Electron. **22**, 390 (2016).
6. J. M. Lee, W. J. Lee, M. S. Kim, and J. J. Ju, J. Lightwave Technol. **37**, 5428 (2019).
7. M. Piekarek, D. Bonneau, S. Miki, T. Yamashita, M. Fujiwara, M. Sasaki, H. Terai, M. G. Tanner, C. M. Natarajan, R. H. Hadfield, J. L. O'Brien, and M. G. Thompson, Opt. Lett. **42**, 815 (2017).
8. Y. Zhao, X. Wang, D. Gao, J. Dong, and X. Zhang, Front. Optoelectron. **12**, 148 (2019).
9. Y. H. Ding, M. H. Pu, L. Liu, J. Xu, C. Peucheret, X. L. Zhang, D. X. Huang, and H. Y. Ou, Opt. Express **19**, 6462 (2011).
10. S. Ibrahim, N. K. Fontaine, S. S. Djordjevic, B. B. Guan, T. H. Su, S. Cheung, R. P. Scott, A. T. Pomerene, L. L. Seaford, C. M. Hill, S. Danziger, Z. Ding, K. Okamoto, and S. J. B. Yoo, Opt. Express **19**, 13245 (2011).
11. P. Orlandi, C. Ferrari, M. J. Strain, A. Canciamilla, F. Morichetti, M. Sorel, P. Bassi, and A. Melloni, Opt. Lett. **37**, 3669 (2012).
12. P. Alipour, A. A. Eftekhar, A. H. Atabaki, Q. Li, S. Yegnanarayanan, C. K. Madsen, and A. Adibi, Opt. Express **19**, 15899 (2011).
13. P. Dong, N. N. Feng, D. Z. Feng, W. Qian, H. Liang, D. C. Lee, B. J. Luff, T. Banwell, A. Agarwal, P. Toliver, R. Menendez, T. K. Woodward, and M. Asghari, Opt. Express **18**, 23784 (2010).
14. X. S. Luo, J. F. Song, S. Q. Feng, A. W. Poon, T. Y. Liow, M. B. Yu, G. Q. Lo, and D. L. Kwong, IEEE Photon. Technol. Lett. **24**, 821 (2012).
15. F. N. Xia, M. Rooks, L. Sekaric, and Y. Vlasov, Opt. Express **15**, 11934 (2007).
16. Z. Cheng, J. Dong, and X. Zhang, Opt. Lett. **45**, 2363 (2020).
17. S. Fan, W. Suh, and J. D. Joannopoulos, J. Opt. Soc. Am. A **20**, 569 (2003).
18. A. Yariv, Y. Xu, R. K. Lee, and A. Scherer, Opt. Lett. **24**, 711 (1999).
19. J. K. S. Poon, J. Scheuer, Y. Xu, and A. Yariv, J. Opt. Soc. Am. B **21**, 1665 (2004).
20. R. R. Kumar, X. R. Wu, and H. K. Tsang, Opt. Lett. **45**, 1289 (2020).
21. R. R. Kumar and H. K. Tsang, Opt. Lett. **46**, 134 (2021).
22. D. Oser, S. Tanzilli, F. Mazeas, C. Alonso-Ramos, X. Le Roux, G. Sauder, X. Hua, O. Alibart, L. Vivien, É. Cassan, and L. Labonté, npj Quantum Inf. **6**, 31 (2020).